Design of Miniature Planar Antennas for 5G Systems

Bousalah Fayza[1]

[1]Telecommunication Department, Université Abou-Bekr Belkaid

November 28, 2022

Advances in Wireless Communications and Networks
2021; 7(1): 1-8
http://www.sciencepublishinggroup.com/j/awcn
doi: 10.11648/j.awcn.20210701.11
ISSN: 2575-5951 (Print); ISSN: 2575-596X (Online)

Design of Miniature Planar Antennas for 5G Systems

Bousalah Fayza

Telecommunication Department, Université Abou-Bekr Belkaid, Tlemcen, Algeria

Received: November 26, 2020; **Accepted**: December 22, 2020; **Published**: April 7, 2021

Abstract: The objective of this work is the design and simulation of an antenna based on metamaterials in order to miniaturize the dimensions of planar antennas. Metamaterials have been on the rise in recent years. The new properties make it possible to envisage the realization of new electronic components with new functions. Metamaterials are artificial materials designed for different telecommunications applications in order to improve the performance of antennas in terms of efficiency, compactness and miniaturization of structures. The use of these materials offers advantages such as reduction in weight and bulk, which is beneficial for their integration into 5G telecommunications and telephony systems. The fifth generation 5G mobile network is a set of emerging global telecommunications standards, typically using high frequency spectrum, to provide network connectivity with reduced latency and higher speed and capacity than the forerunners. It is argued that the recurring communication infrastructure is very inefficient in energy and that 5G should be designed to solve this problem, increasing energy efficiency by several orders of magnitude. To meet the demands of 5G, we need radically new network architectures and technologies, such as heterogeneous ultra-dense network, massive multi-output MIMO, and millimeter wave communications. Our goal is to achieve a planar antenna based on metamaterials which must operate at the resonance frequency of 5G which is f=3.5GHz by the CST Studio Suit electromagnetic design and simulation software and Matlab calculation.

Keywords: Planar Antenna, Patch Antenna, Metamaterials, SRR, CSRR, Millimeter Band, 5G Systems, Ansoft HFSS, CST-MWS, Matlab

1. Introduction

In order to miniaturize planar antennas; we used miniaturization techniques based on metamaterial technologies. These have been gaining momentum in recent years [1, 2]. The use of these materials offers advantages such as reduction in weight and bulk, which is beneficial for their integration into electronic systems such as telecommunications systems for 5G [3]. Our work consists of giving an overview on planar antennas and the mechanism of their operations based on metamaterials, we will propose a design approach for a patch antenna deposited on a monolayer substrate by placing a CSRR cell based on it above. metamaterials working in millimeter wave. Subsequently, we will do a synthesis study to extract the various parameters influencing its electromagnetic behavior. The studied and designed antenna is intended to be used for 5G [4] telecommunications and telephone applications in the [3.3-3.8] GHz frequency band.

This article presents a concrete case of the design of a rectangular printed antenna, in order to study, design, simulate, characterize and analyze the various parameters of this antenna. This project consists of developing antennas capable of radiating at the frequency of 3.5 GHz, which could be used in a very large number of applications of telecommunications systems currently for 5G [5, 6].

The objective of our work is to miniaturize the dimensions of the initial planar antenna in order to understand the influences of the square CSRR complementary split-ring resonator cells on the planar antennas. First, we modeled and designed the rectangular patch antenna from the dimensions obtained by Maxwell's electromagnetic equations under the Matlab environment. Next, we applied the CSRR cells on the patch antenna to make a parametric study of the different geometric shapes and locations of the CSRR cells on the patch and the ground plane. The various results of simulations of the “S11” reflection and “S21” transmission coefficients are obtained by the electromagnetic software CST are satisfactory and promising.

2. Characteristics of Planar Antennas

The principle is to design a patch antenna which must operate at the resonant frequency 3.5 GHz, with a reflection coefficient of less than -10dB. The principle is to design a patch antenna which must operate at the resonant frequency 3.5 GHz, with a reflection coefficient of less than -10dB. To perform the various calculations of the dimensions of the rectangular patch antenna, we used the permittivity of the substrate εr=4.3 with a thickness of h=1.56mm [7, 8].

2.1. Theoretical Calculations of the Dimensions of the Rectangular Patch Antenna

The values characterizing the different elements of the antenna are given as follows:

1. Dielectric permittivity of the substrate (FR-4 "Fire Retardant"): εr=4.3
2. Height of dielectric substrate: hs=1.56mm
3. Desired resonance frequency (5G): fr=3.5 GHz
4. Adaptation to 50 Ohm
5. Power supply by microstrip line
6. Metallization thickness: h=0.035mm

To perform the various calculations of the dimensions of the rectangular patch antenna, we used the permittivity of the substrate εr=4.3 with a thickness of h=1.56mm.

1) Calculate the patch width Wp:

$$Wp= \qquad (1)$$

2) Calculation of effective dielectric constant εreff:

$$= + \quad 1\ 12 \qquad (2)$$

3) Calculate the effective length:

$$Leff= \sqrt{\quad} \qquad (3)$$

4) Extension length (ΔL):

$$\Delta \quad 0.412*h* \qquad (4)$$

5) Calculate the patch length (Lp):

$$Lp=L_{eff}-2*\Delta, \qquad (5)$$

6) Feed length calculation (LL):

$$LL= \qquad (6)$$

7) Calculation of substrate length (Lg):

$$Lg=Lp+6*h+LL \qquad (7)$$

8) Calculate the width of the substrate (Wg):

$$Wg=Wp+6*h \qquad (8)$$

9) Dimension of the transmission line - 3.05822. Table 1 shows the different parameters of the patch antenna.

Table 1. *Dimensions of the patch antenna parameters.*

26.32	3.9214	12.75	0.6915	20.40	42	71.76	35.058

2.2. Design and Simulation Results of the Rectangular Patch Antenna with Notches

Figure 1a shows a rectangular patch antenna with notches, the latter are used for better adaptation of the antenna to the resonant frequency 3.5GHz. Figure 1b gives the simulation result of the reflection coefficient S11=-29dB as a function of the frequency f=3.51GHz. Figure 1c shows the radiation pattern of the antenna. Figure 1d represents the directivity of the antenna, the angles phi=90° and Theta=270° with a gain of 6.2dB, which shows that the antenna is directional.

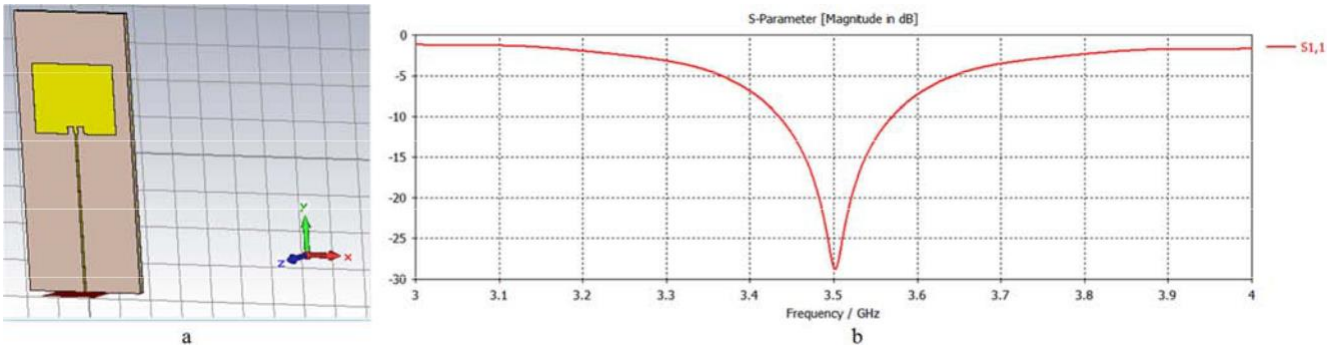

a b

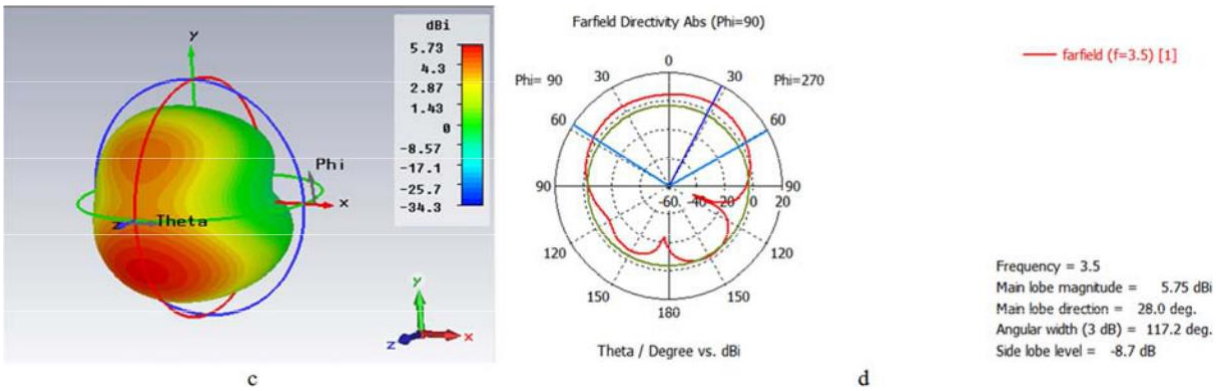

Figure 1. *a. Representation of a rectangular patch antenna with notches. b. Reflection coefficient S11 as a function of frequency. c. Patch antenna gain radiation pattern with notches. d. Patch antenna directivity diagram with notches.*

3. Design and Simulation of Metamaterial Cells

3.1. Design and Simulation of the SRR Cell

Figure 2 shows the SRR cell and its reflection coefficient S11 as a function of the resonant frequency of the patch antenna. The different dimensions of the SRR are given in Table 1 [9].

Table 2. *Dimensions of the SRR.*

Substrate length Ls	Substrate height Hs	Spacing between rings S	S Ring thickness W
5.55mm	1.56 mm	0.15 mm	0.2 mm

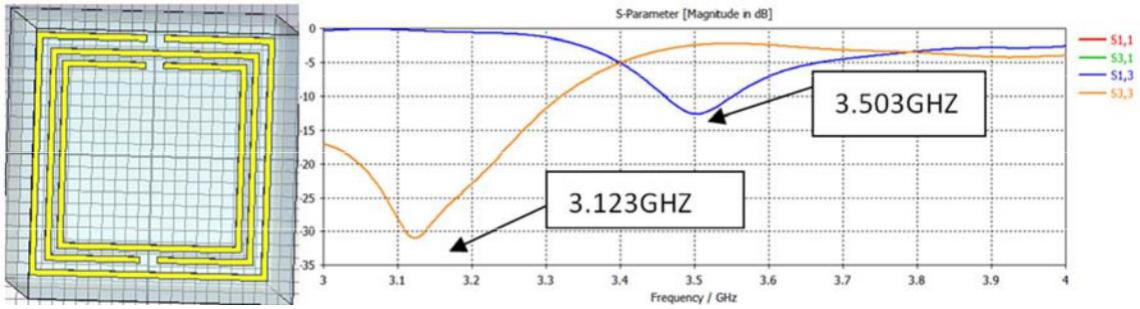

Figure 2. *Representation of a 3-ring SRR unit with opposite openings and its S-parameters.*

Figure 2 shows the evolution of the S11 reflection and S21 transmission coefficients as a function of the resonant frequency of the SRR [10]. We notice that the designed SRR has a transmission lower than -14dB for a frequency of 3.50GHz and a reflection coefficient of -30.96dB for a frequency of 3.123GHz.

3.2. Design and Simulation of the CSRR Cell with 3 Rings with Opposite Openings

Figure 3 shows the 3-ring CSRR cell with opposite openings. The 3 concentric interrupted metallic rings (copper) engraved on a dielectric support (Substrate) [11].

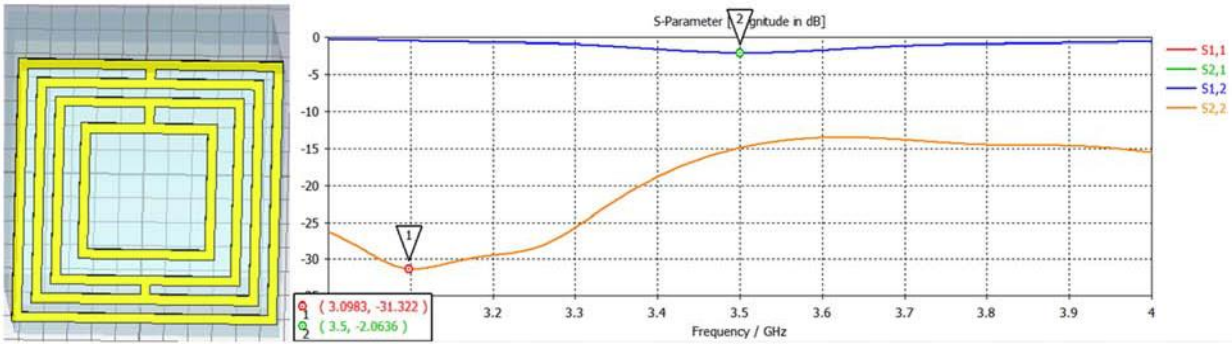

Figure 3. *Representation of a 3-ring CSRR unit with opposite openings and its S-parameters.*

We notice that the CSRR presents a reflection coefficient S11 of -31dB for a frequency of 3.104 GHz and a transmission S21 of -2.06 dB for a frequency of 3.5GHz, according to figure 3.

Table 3. *Values of the reflection coefficients for different patch antennas with different positions and numbers of CSRR cells on patch and ground plane.*

CSRR position on patch and PDM	Fréquency (GHz)	S-Paramèters (dB)
2 CSRR verticals on patch	3.269	-28.467
2 CSRR horizontals on patch	3.417	-27.23
2 CSRR verticals on PDM	3.212	-37.13
1 CSRR on patch	3.288	-29.66
1CSRR on PDM	3.45	-25.69

3.3. Interpretation of Simulation Results Before Adaptation

The parameters of the different antenna configurations depending on the number and the position of the CSRR cells used in table 3. This table represents the different positions and numbers of CSRR cells engraved on the patch and ground plane or both at the same time with the resonant frequency and the reflection coefficient (S11).

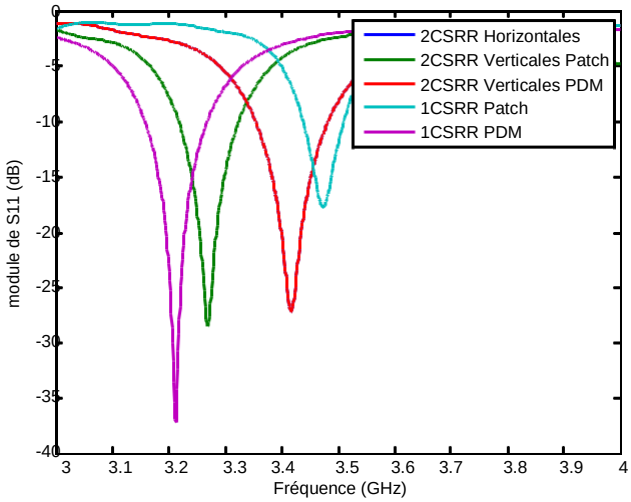

Figure 4. *Coefficient S11 as a function of frequencies for different antennas loaded with 3-ring CSRRs with opposite openings before adaptation.*

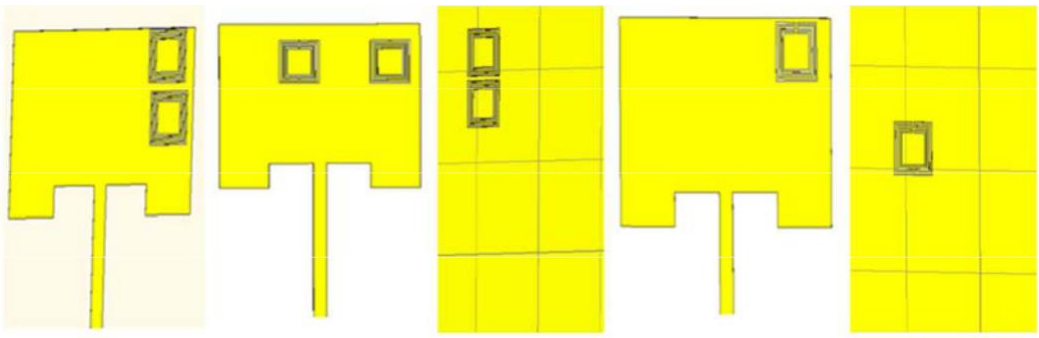

Figure 5. *Representation of patch antennas loaded with CSRR with 3 rings with opposite openings.*

Table 4. *Values of the reflection coefficients for different patch antennas with different positions of CSRR cells on patch and ground plane.*

CSRR position on patch and PDM	Fréquency (GHz)	S-Paramèters (dB)
2 CSRR verticals on patch	3.509	-28.20
2 CSRR horizontals on patch	3.506	-29.79
1 CSRR on PDM	3.45	-25.69
1 CSRR on patch	3.501	-30.088

3.4. Interpretation of Antenna Simulation Results After Adaptation

The parameters of the different antenna configurations depending on the number and position of CSRR cells used are presented in Table 4 which shows the position of the CSRR cells on the patch or the ground plane (PDM) with the resonant frequency and the reflection coefficient (S11).

The results of the S parameters of the previous antennas show band-cut behavior at the 3.5 GHz frequency, corresponding to the resonant frequency of the CSRR cell after optimization and modification of the antenna parameters.

The best optimizations for the different positions of the CSRR cells with their miniaturization rates, their efficiencies and their bandwidth widths are given in Table 5 at the frequency 3.5GHz.

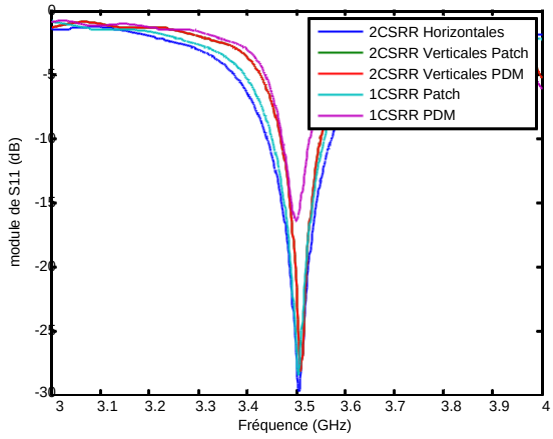

Figure 6. *Coefficient S11 as a function of frequencies for different antennas loaded with 3 ring CSRRs with opposite openings after adaptation.*

Table 5. *Values of miniaturization rates, yields and bandwidths for the different antennas with CSRR engraved on patch and / or PDM.*

CSRR position on patch and PDM	Miniaturization rate (%)	efficiency (%)	Bandwidth (%)
2 CSRR verticals on patch	18.5	2.28	8
2 CSRR horizontals on patch	18.58	3.7	13
1 CSRR on PDM	Pas d'adaptation	1.99	7.2
1 CSRR on patch	13.79	2.57	9
2 CSRR verticals on PDM and patch	Pas d'adaptation	2.3	7.15

Table 6 shows the parameters of the patch antenna after adaptation.

Table 6. *Parameters of the patch antenna after adaptation.*

CSRR position on patch	Wp (mm)	Lp (mm)	Wg (mm)	Lg (mm)
2 CSRR verticals on patch	25.6	18.04	35.65	76
2 CSRR horizontals on patch	25.7	19.945	35.65	76
1 CSRR on PDM	28	20.26	35.65	72.74
1 CSRR on patch	26.68	18.333	35.8	79.88
2 CSRR vertical on PDM and patch	28	20.26	35.65	72.74

3.5. Interpretation of Antenna Simulation Results After Adaptation

The gain values before and after adaptation for the different antenna configurations depending on the number and position of the CSRR cells are presented in Table 7.

Table 7. *Values of the gain of the patch antenna before and after adaptation.*

CSRR position on patch and PDM	Gain before adaptation	Gain after adaptation
2 CSRR verticals on patch	6.1	5.9
2 CSRR horizontals on patch	6.21	5.97
2 CSRR verticales on PDM	5.61	5.61
1 CSRR on patch	5.33	5.33
1 CSRR on PDM	6.14	6.14

After simulating the different patch antennas with different positions and numbers of CSRR cells on patch or ground plane or on both sides of the antennas at the same time, we notice that the gain values obtained before adaptation of the antennas are higher than those after adaptation.

3.6. Comments Before and After Adaptation of the Patch Antenna

Table 8. *Comments on the figures.*

CSRR position on patch and PDM	Before adaptation	After adaptation
2 CSRR verticals on patch	Very good reduction in frequency to 3.269GHz with a reflection coefficient of -28.46dB Resonance frequency and desired reflection coefficient -31dB better optimization.	Resonance frequency and desired reflection coefficient -31dB better optimization.
2 CSRR horizontales sur patch	Reduction of the frequency to 3.41GHz with a coefficient of -27.23dB Good optimization of the resonant frequency and desired reflection coefficient	Good optimization of the resonant frequency and desired reflection coefficient
2CSRR sur patch et PDM	Despite the frequency decrease to 3.47GHz the reflection coefficient is very far -17dB. Desired frequency of 3.5GHZ with a good reflection coefficient of -30dB.	Desired frequency of 3.5GHZ with a good reflection coefficient of -30dB.
1CSRR sur PDM	A resonant frequency reduced to 3.45Ghz with a low reflection coefficient at -25.69dB Close to the resonant frequency but the very low reflection coefficient -23dB.	Close to the resonant frequency but the reflection coefficient very low -23dB.

4. Design and Simulation of 3-ring SRR and CSRR Cells with Openings in the Same Direction

Figure 7 shows the SRR cell. with 3 rings with openings in the same direction and the results of simulations of the S-parameters.

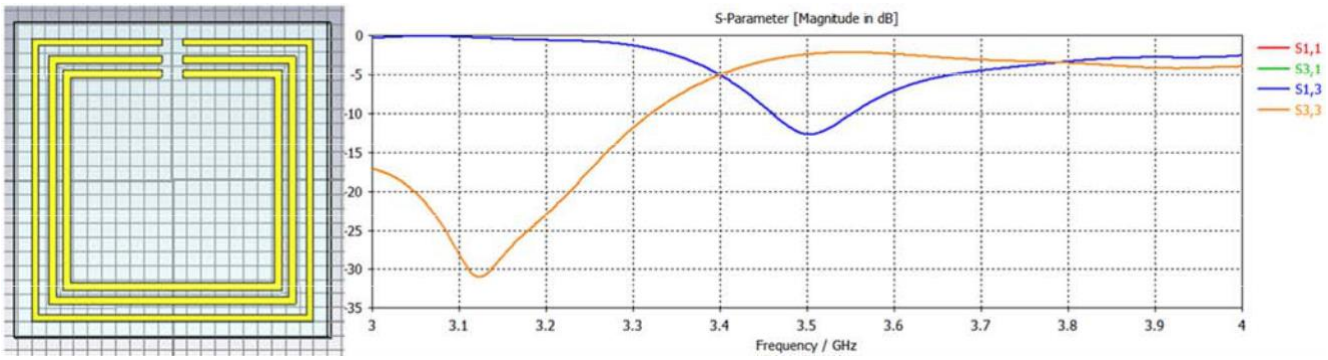

***Figure 7**. Representation of the 3-ring SRR with openings in the same direction.*

Figure 7 illustrates the evolution of coefficients S11 and S21 as a function of the frequency of the SRR. We notice that the transmission coefficient is -15dB at the frequency 3.5GHz and a reflection coefficient of -30.91dB at the frequency 3.113GHz.

4.1. Design and Simulation of the 3-ring CSRR Cell with Openings in the Same Direction

Figure 8 shows the 3-ring CSRR with openings in the same direction. The 3 concentric interrupted metal rings are etched on a dielectric support (substrate).

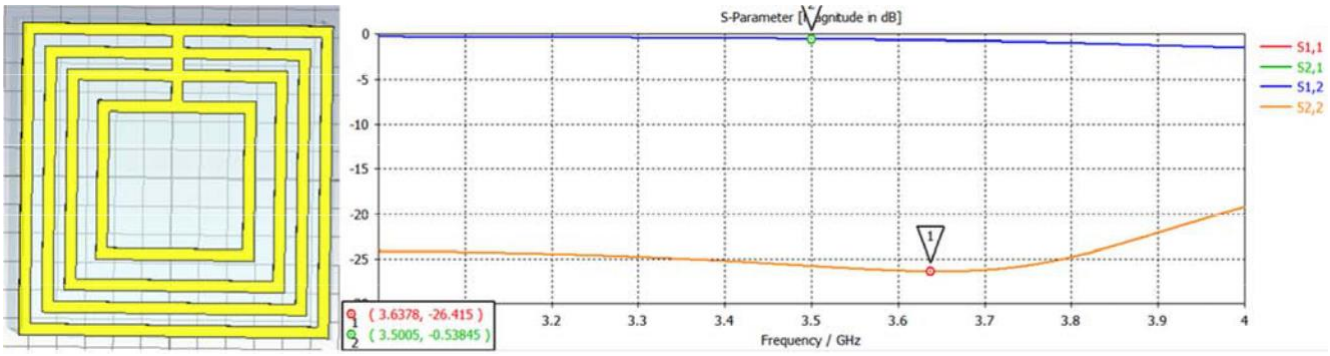

***Figure 8.** Representation of the 3-ring CSRR with openings in the same direction and the different -S parameters.*

***Table 9.** Value of the reflection coefficient for the patch antenna with position of the 3 ring CSRR cell with openings in the same direction before adaptation.*

CSRR position on patch	Fréquency (GHz)	S-Paramèters (dB)
1 CSRR with 3 rings with openings in the same direction	3.288	-29.66

We notice that the CSRR has a transmission coefficient S21 of -2.07dB at 3.5GHz.

4.2. Interpretation of Simulation Results Before Adaptation

The parameters of the different antenna configurations depending on the number and position of CSRR cells used are shown in the table which shows the position of the CSRR cells on the patch with the resonant frequency and the reflection coefficient (S11).

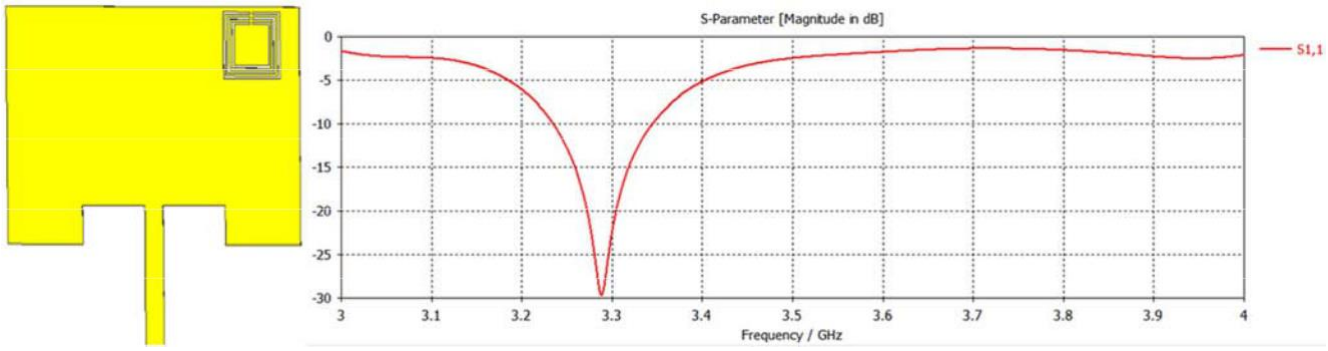

***Figure 9.** Patch antenna with 1 CSRR and its coefficient S11 as a function of frequency.*

4.3. Interpretation of Antenna Simulation Results After Adaptation

The parameters of the different antenna configurations depending on the number and position of CSRR cells depending on the frequency and the reflection coefficient (S11) are shown in Table 10.

Table 10. *Value of the reflection coefficient for a patch antenna with 3-ring CSRR cell position with openings in the same direction after adaptation.*

CSRR position on patch	Fréquency (GHz)	S-Paramèters (dB)
1 CSRR with 3 rings with openings in the same direction.	3.501	-30.088

The results of the S parameters in the previous figures show band-cut behavior around 3.5 GHz, corresponding to the resonant frequency of the CSRR cell after optimization and modification of the antenna parameters.

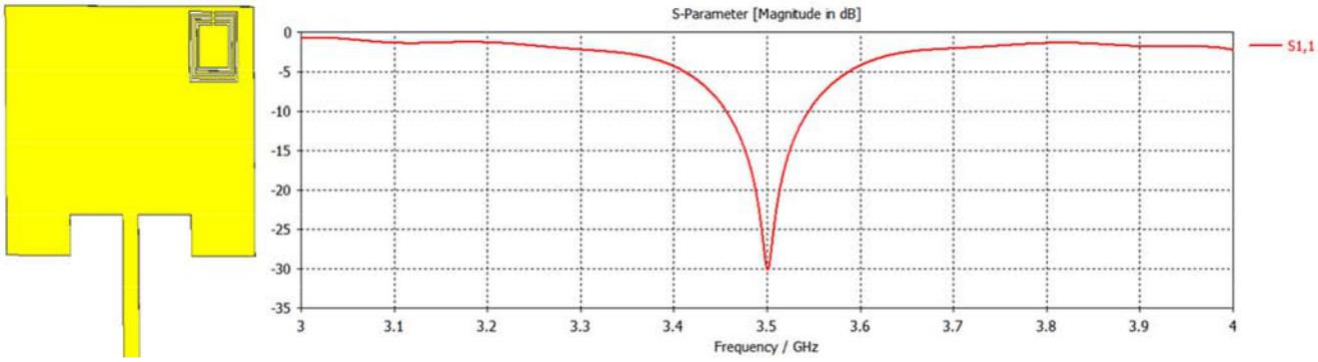

Figure 10. *Patch antenna with 1 CSRR and its coefficient S11 as a function of frequency.*

The best optimizations obtained from the different positions and numbers of CSRR cells with their miniaturization rates, efficiencies and bandwidth widths are given in Table 11.

Table 11. *Value of the miniaturization rate, the efficiency and the bandwidth for a patch antenna with 3-ring CSRR with openings in the same direction.*

CSRR position on patch	Miniaturization rate (%)	efficiency (%)	Bandwidth (%)
1 CSRR with 3 rings with openings in the same direction	13.79	2.57	9

Table 12 shows the new parameters of the patch antenna after adaptation.

Table 12. *Parameter of the patch antenna after adaptation.*

CSRR position on patch	Wp (mm)	Lp (mm)	Wg (mm)	Lg (mm)
1 CSRR with 3 rings with openings in the same direction	26.68	18.333	35.8	79.88

4.4. Interpretation of the Gain Results Before and After Adaptation

The gain values for this antenna configuration as a function of the positions of the CSRRs are shown in Table 13 which represents the position of the 3-ring CSRR cells with openings in the same direction on the patch and the gain values before and after adaptation.

Table 13. *Values of the gain of the patch antenna before and after adaptation.*

CSRR position on patch	Gain before adaptation	Gain after adaptation
1 CSRR with 3 rings with openings in the same direction	6.09	5.7

After simulation of patch antennas with different positions and number of CSRR cells on patch, we notice that the gain values before adaptation of the antennas are higher than those obtained after adaptation.

4.5. Comments Before and After Adaptation

Table 14. *Comments on the figures.*

CSRR position on patch	Before adaptation	After adaptation
1 CSRR with 3 rings with openings in the same direction	Very good frequency reduction at 3.288GHZ with a coefficient of -29.66dB.	Desired resonance frequency of 3.501GHZ with a good coefficient S11=-30.88dB.

5. Conclusion

It was possible to model a patch antenna using the electromagnetic software Microwave Studio (CST). This modeling made it possible to study the influence of various parameters of the rectangular patch antenna radiation patterns for 5G applications.

The design of the different patch antennas loaded with 3-ring CSRR metamaterial resonators with opposite openings and openings in the same direction are set to have a good response at the resonant frequency of 3.5 GHz. The resonance response of these structures varies according to the number and the position of the CSRR resonators, whether on the patch or on the ground plane.

Subsequently, we confirmed that the choice of the position and the number of cells relative to the antenna, is an important condition in order to optimize the level of coupling and to ensure the desired metamaterial effect. The simulation results obtained confirm the obtaining of a better result of reflection coefficients, miniaturization rate, efficiency and gain at the frequency 3.5 GHz for the antennas loaded with 3-ring CSRRs with opposite apertures. The bandwidth varies from 83 MHz to 94 MHz with a reflection coefficient that varies between -25.7 dB and -37.8 dB, depending on the position and number of CSRRs on the antenna.

The goal of this work is to miniaturize patch antennas using CSRR cells embedded on the patch or on the ground plane. Antenna miniaturization technology minimizes the cost and also the gain in materials and surfaces to be used.

References

1. Ghillani, D. (2022). Deep Learning and Artificial Intelligence Framework to Improve the Cyber Security. *Authorea Preprints*.
2. Ghelani, D. (2022). Cyber Security, Cyber Threats, Implications and Future Perspectives: A Review. *Authorea Preprints*.
3. Ghelani, D., Hua, T. K., & Koduru, S. K. R. (2022). Cyber Security Threats, Vulnerabilities, and Security Solutions Models in Banking. *Authorea Preprints*.
4. Ghelani, D. (2022). Digital Educational Coordination System (DECS).
5. Ghelani, D. (2022). What is Non-fungible token (NFT)? A short discussion about NFT Terms used in NFT. *Authorea Preprints*.
6. Ghelani, D., & Faisal, S. (2022). Synthesis and characterization of Aluminium Oxide nanoparticles. *Authorea Preprints*.
7. Koricanac, I. (2021). Impact of AI on the Automobile Industry in the US. *Available at SSRN 3841426*.
8. Hua, T. K. (2022). A Short Review on Machine Learning. *Authorea Preprints*.
9. Hua, T. K. (2022). Cybersecurity As A Fishing Game.
10. Ghelani, D., & Hua, T. K. A Perspective Review on Online Food Shop Management System and Impacts on Business.
11. Ilyes, A., Mohammed Djamel Edine, B., & Said, B. (2015). *Development of a smart irrigation system* (Doctoral dissertation, UNIVERSITY OF KASDI MERBAH OUARGLA).
12. Achar, S. (2015). Requirement of Cloud Analytics and Distributed Cloud Computing: An Initial Overview. *International Journal of Reciprocal Symmetry and Physical Sciences*, *2*(1), 12-18.
13. Achar, S. (2017). Asthma Patients' Cloud-Based Health Tracking and Monitoring System in Designed Flashpoint. *Malaysian Journal of Medical and Biological Research*, *4*(2), 159-166.
14. Achar, S. (2022). Cloud Computing Forensics. *International Journal of Computer Engineering and Technology*, *13*(3).
15. Achar, S. (2022). Cloud Computing Security for Multi-Cloud Service Providers: Controls and Techniques in our Modern Threat Landscape. *International Journal of Computer and Systems Engineering*, *16*(9), 379-384.
16. Achar, S. (2022). Cloud Computing Security for Multi-Cloud Service Providers: Controls and Techniques in our Modern Threat Landscape. *International*

Journal of Computer and Systems Engineering, *16*(9), 379-384.

17. Achar, S. (2019). Early Consequences Regarding the Impact of Artificial Intelligence on International Trade. *American Journal of Trade and Policy*, *6*(3), 119-126.
18. Achar, S. (2016). Software as a Service (SaaS) as Cloud Computing: Security and Risk vs. Technological Complexity. Engineering International, 4 (2), 79-88.
19. Achar, S. (2020). Influence of IoT Technology on Environmental Monitoring. *Asia Pacific Journal of Energy and Environment*, *7*(2), 87-92.
20. Achar, S. (2019). Cloud-based System Design. *International Journal of All Research Education and Scientific Methods (IJARESM)*, *7*(8), 23-30.
21. Achar, S. (2016). Software as a Service (SaaS) as Cloud Computing: Security and Risk vs. Technological Complexity. *Engineering International*, *4*(2), 79-88.
22. Achar, S. (2022). How Adopting A Cloud-Based Architecture Has Reduced The Energy Consumptions Levels. *International Journal of Information Technology and Management*, *13*(1), 15-23.
23. Achar, S. (2021). An Overview of Environmental Scalability and Security in Hybrid Cloud Infrastructure Designs. *Asia Pacific Journal of Energy and Environment*, *8*(2), 39-46.
24. Achar, S. (2020). Cloud and HPC Headway for Next-Generation Management of Projects and Technologies. Asian.
25. Achar, S. (2018). Security of Accounting Data in Cloud Computing: A Conceptual Review. *Asian Accounting and Auditing Advancement*, *9*(1), 6072.
26. Achar, S. (2022). CLOUD COMPUTING: TOWARD SUSTAINABLE PROCESSES AND BETTER ENVIRONMENTAL IMPACT. *Journal of Computer Hardware Engineering (JCHE)*, *1*(1).
27. ACHAR, S., PATEL, H., & HUSSAIN, S. (2022). DATA SECURITY IN CLOUD: A REVIEW. *Asian Journal of Advances in Research*, *17*(4), 76-83.
28. Achar, S. A Comprehensive Study of Current and Future Trends in Cloud Forensics.
29. Achar, S. (2021). Enterprise SaaS Workloads on New-Generation Infrastructure-as-Code (IaC) on Multi-Cloud Platforms. *Global Disclosure of Economics and Business*, *10*(2), 55-74.
30. Achar, S. (2020). Maximizing the Potential of Artificial Intelligence to Perform Evaluations in Ungauged Washbowls. Engineering International, 8 (2), 159-164.
31. Abcouwer, T., Takács, E., & Rácz, C. (2021, November). Innovating Management and Leadership in Contemporary Times: Motivation and Evaluation in Learning. In *ECMLG 2021 17th European Conference on Management, Leadership and Governance* (p. 1). Academic Conferences limited.
32. Chimakurthi, V. N. S. S. (2017). Cloud Security-A Semantic Approach in End to End Security Compliance. Engineering International, 5 (2), 97106.
33. Chimakurthi, V. N. S. S. (2018). Emerging of Virtual Reality (VR) Technology in Education and Training. *Asian Journal of Humanity, Art and Literature*, *5*(2), 157-166.
34. Chimakurthi, V. N. S. S. (2017). Cloud Security-A Semantic Approach in End to End Security Compliance. *Engineering International*, *5*(2), 97106.
35. Chimakurthi, V. N. S. S. (2019). Implementation of Artificial Intelligence Policy in the Field of Livestock and Dairy Farm. *American Journal of Trade and Policy*, *6*(3), 113-118.
36. Chimakurthi, V. N. S. S. (2017). Risks of MultiCloud Environment: Micro Services Based

Architecture and Potential Challenges. *ABC Research Alert*, *5*(3), States-States.

37. Chimakurthi, V. N. S. S. (2020). Digital Asset Management in the Communication of Product Promotional Activities. *Asian Business Review*, *10*(3), 177-186.
38. Chimakurthi, V. N. S. S. (2021). The Future of Cloud Computing Amidst A Desperate Security
39. Maze: The Impact Of COVID And The Future Challenges. *Asian Journal of Humanity, Art and Literature*, *8*(2), 75-84.
40. Chimakurthi, V. N. S. S. (2019). Application Portfolio Profiling and Appraisal as Part of Enterprise Adoption of Cloud Computing. *Global Disclosure of Economics and Business*, *8*(2), 129142.
41. Chimakurthi, V. N. S. S. (2021). An Optimal Cloud Based Electric Vehicle Charging System. *Asia Pacific Journal of Energy and Environment*, *8*(2), 29-38.
42. Chimakurthi, V. N. S. S. (2020). Digital Asset Management: A Lowdown on Intricacies of Digital Rights and Permissions. *Global Disclosure of Economics and Business*, *9*(2), 129-140.
43. Chimakurthi, V. N. S. S. (2019). Efficacy of Augmented Reality in Medical Education. *Malaysian Journal of Medical and Biological Research*, *6*(2), 135-142.
44. Chimakurthi, V. N. S. S. (2021). Strategic Growth of Everything-as-a-Service (XaaS) Business Model Transformation. *Engineering International*, *9*(2), 129-140.
45. Chimakurthi, V. N. S. S. (2020). Application of Convolution Neural Network for Digital Image Processing. *Engineering International*, *8*(2), 149158.
46. Chimakurthi, V. N. S. S. (2020). The Challenge of Achieving Zero Trust Remote Access in MultiCloud Environment. *ABC Journal of Advanced Research*, *9*(2), 89-102.
47. Reddy, P., Srianirudh, K. T., Kumar, K. U., Gondela, H. S. K., & Surendhra, V. N. S. (2009, March). Trajectory Prediction and Data Filtering for Mobile Networks. In *2009 International Conference on Future Networks* (pp. 263-267). IEEE.